Accepted Manuscript

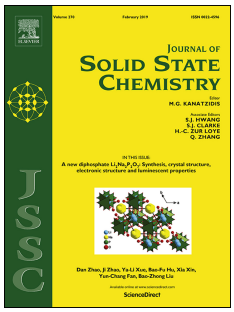

The first hafnium germanate with garnet-type of structure: Mild hydrothermal synthesis, crystal structure and new mechanism of hydroxyl inclusion

Stanislav Ferdov, Zhi Lin

PII: S0022-4596(19)30086-6

DOI: https://doi.org/10.1016/j.jssc.2019.02.031

Reference: YJSSC 20630

To appear in: *Journal of Solid State Chemistry*

Received Date: 11 January 2019

Revised Date: 14 February 2019

Accepted Date: 20 February 2019

Please cite this article as: S. Ferdov, Z. Lin, The first hafnium germanate with garnet-type of structure: Mild hydrothermal synthesis, crystal structure and new mechanism of hydroxyl inclusion, *Journal of Solid State Chemistry* (2019), doi: https://doi.org/10.1016/j.jssc.2019.02.031.

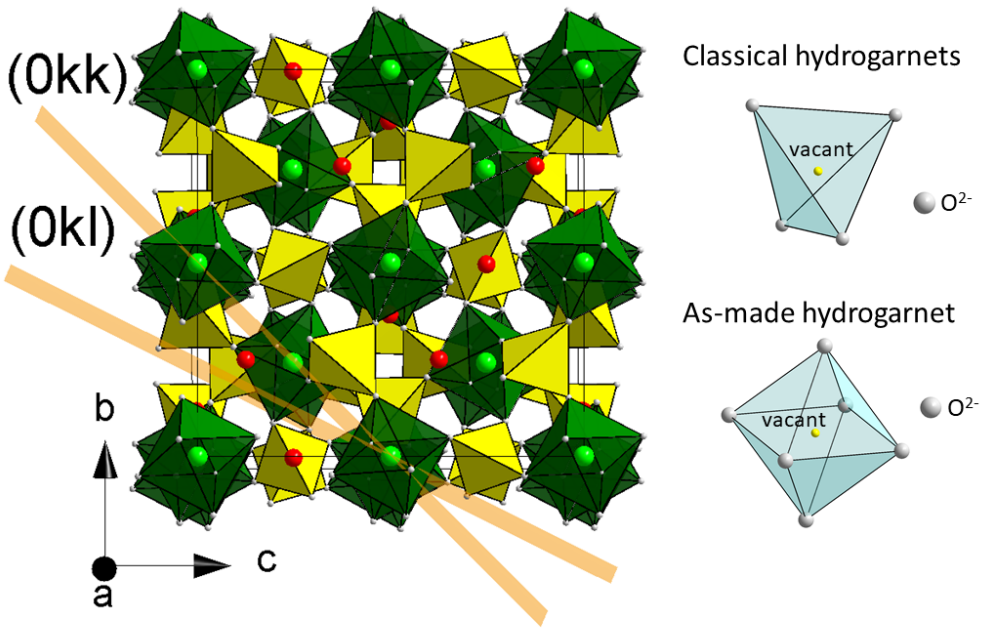

The first hafnium germanate with garnet-type of structure: mild hydrothermal synthesis, crystal structure and new mechanism of hydroxyl inclusion

Stanislav Ferdov[1,*] and Zhi Lin[2]

[1]Department of Physics, University of Minho, 4800-058 Guimarães, Portugal

[2]CICECO, Department of Chemistry, University of Aveiro, 3810-193 Portugal

Correspondence e-mail: sferdov@fisica.uminho.pt

Abstract

Sodium hafnium germanate, $Na_3Hf_{1.7}Ge_3O_{10}(OH)_{1.8}$, with garnet-type of structure was synthesized as a single phase, nanoparticles (100-600 nm) at mild hydrothermal conditions (230 ^oC) and autogenous pressure. The structure was solved ab initio from powder X-ray diffraction data and subsequently refined [R_{exp}: 6.10, R_{wp}: 7.26, R_p: 5.39, GOF: 1.19, R_B: 1.50] by the method of Rietveld. The solid crystallizes in cubic space group *Ia*-3*d* (230), with a = 12.6819(2) Å, V = 2039.65(1) Å^3 and Z = 8. The structure is built up of rare combination of two tetravalent (Ge^{4+} and Hf^{4+}) and one monovalent (Na^+) cation alternating in form corner-sharing GeO_4 tetrahedra and HfO_6 octahedra whose negative charge is compensated by Na^+ residing in dodecahedral coordination. Unlike the typical tetrahedral site disorder in hydrogarnets (hydrogrossular, hibschite, and katoite) we found that the octahedral position of the heavy Hf^{4+} cation is partly vacant which reveals alternative mechanism of charge unbalance leading to incorporation of hydroxyl group. Furthermore, the synthesized material is the first hafnium germanate with garnet-type of structure and the second known sodium hafnium germanate.

Keywords: Hafnium garnet; Hydrogarnet; Hydrothermal synthesis; Nanoparticles; Disorder, Hydroxyl inclusion; Crystal structure.

1. Introduction

The garnet supergroup comprises all minerals with a garnet structure independently of the elements that occupy the four sites in the general formula $A_3B_2C_3D_{12}$ (A, B and C correspond to dodecahedral, octahedral, and tetrahedral sites, respectively, and D is O, OH or F) [1]. Garnets are common rock-forming minerals and often referred as a petrochronometer for accurate determination of the age of rocks [2]. Since the discovery of the ferrimagnetic ferrogamets and laser technology the garnet-type of solids became a main stream of fundamental and application research [3-11]. For more than 50 years the elemental diversity of the synthetic garnets was extended far beyond their natural counterparts. In the available literature there are more than 200 different chemical compositions of structurally characterized garnet-type of solids. Among them, germanium-based garnets attract special attention due to their applications as a substrate for magnetic bubble devices [5] and as phosphors in optoelectronic devices [6, 8, 9]. However, with a few exceptions the synthesis of germanium garnets is limited by high-temperature (over 500 ^oC) conditions, co-crystallization with secondary phases and multiple steps of preparation [10-12]. Furthermore, in spite of the widespread occurrences of germanium minerals, long-term research and number of different compositions of germanium materials, there are chemical systems where no germanium garnets have been found. Such a system is Na_2O-GeO_2-HfO_2. Additionally, we found that in the garnet-type of structure the dodecahedral site is rarely occupied only by monovalent sodium cation. The only examples of sodium garnets are: $Na_2MgSi_3O_{12}$ (majorite) [13], $Na_3(Fe,Al)_3Te_2O_{12}$ [14] and $Na_3Zr_{1.8}Ge_3O_{10}(OH)_{2.2}$ [8].

Here we demonstrate the synthesis of $Na_3Hf_{1.7}Ge_3O_{10}(OH)_{1.8}$ which is the first garnet-type of hafnium germanate and the second known hafnium germanate. The structure was solved ab initio from laboratory powder XRD data and refined by the method of Rietveld which revealed unusual mechanism for the formation of hydrogarnets.

2. Experimental

The synthesis of $Na_3Hf_{1.7}Ge_3O_{10}(OH)_{1.8}$ was carried out by mixing two solutions: (1) 1.07 g of NaOH (Aldrich, ≥ 98 %) and 0.56 g of GeO_2 crystalline powder (Aldrich, 99.998 %) were dissolved in 10.26 g of distilled water, and (2) 0.19 g of $HfCl_4$ (Aldrich, 98%) dissolved in 8.37 g of distilled water. The obtained white gel was homogenized for 5 min by magnetic stirrer (500 rpm) and subsequently transferred into Teflon-lined stainless steel autoclave. The crystallization was performed in preheated oven at 230 ^oC for 5 days. The sample was recovered by filtering and subsequently washed by distilled water. Finally, the solid was dried at room temperature for several days. The D_2O treated sample was done as follows. In 3 mL autoclave, the as-synthesized sample was mixed with D_2O and kept in RT for 2 days, then treated at 120 ºC for 4 days. The obtained product was directly dried at 75ºC for 2 hours before the measurement of FTIR.

Powder XRD pattern was collected at room temperature using a Bruker D8 diffractometer operating with Cu $K\alpha_{1,2}$ *X*-radiation (λ_1 = 1.540596 Å; λ_2 = 1.544493 Å) (X-ray tube operating at 40 kV, 40 mA), filtered by Ni foil. Intensity data were recorded in θ-2θ step scan mode in the 10-140 ^{o} 2θ range (step 0.04^o and time 10 s) from powder sample packed in a flat plate holder. The indexing of the powder XRD pattern, analysis of the systematic absences (N-TREOR software) [15] and structure solution (direct methods of SIRPOW) were carried out via the software package eXpo2004 [16]. After subtraction of the background, the structure factor

amplitudes were extracted by the method of Le Bail [17] using Pearson profile functions along the whole angular interval. The location of the Hf, Ge and O atoms was determined directly while additional difference Fourier syntheses were employed in order to localize the Na atom. The obtained unit cell, space group and atomic coordinates were used as a starting model for the Rietveld refinement (software TOPAS-3; Bruker AXS, Karlsruhe, Germany). The profile fitting (Fig. 1a) was performed by the fundamental parameter approach (FPA) applying full axial model along the entire 2θ range, including sample and instrument dependent parameters such as zero shift, scale factor, unit cell, background (Chebychev polynomial fitting), positions of fractional atomic coordinates, site occupancy factors (Na, Ge and Hf) and isotropic displacement parameters (Tables 1, S1 and supplementary cif file).

The scanning electron microscopy images (SEM) and energy-dispersive X-ray spectroscopy (EDS) chemical analysis were performed by NanoSEM - FEI Nova 200 (FEG/SEM) and EDAX - Pegasus X4M (EDS/EBSD), respectively. Fourier transform infrared (FTIR) spectra of powdered samples suspended in KBr pallets were collected in the range of 400 - 4000 cm^{-1} using a Mattson Mod 7000 spectrometer, resolution 2 cm^{-1}. Differential scanning calorimetry (DSC) and thermogravimetry (TG) curves were measured with Shimadzu DSC-50 or TGA-50 analyzers. The samples were heated under air at a rate of 5 ºC/min.

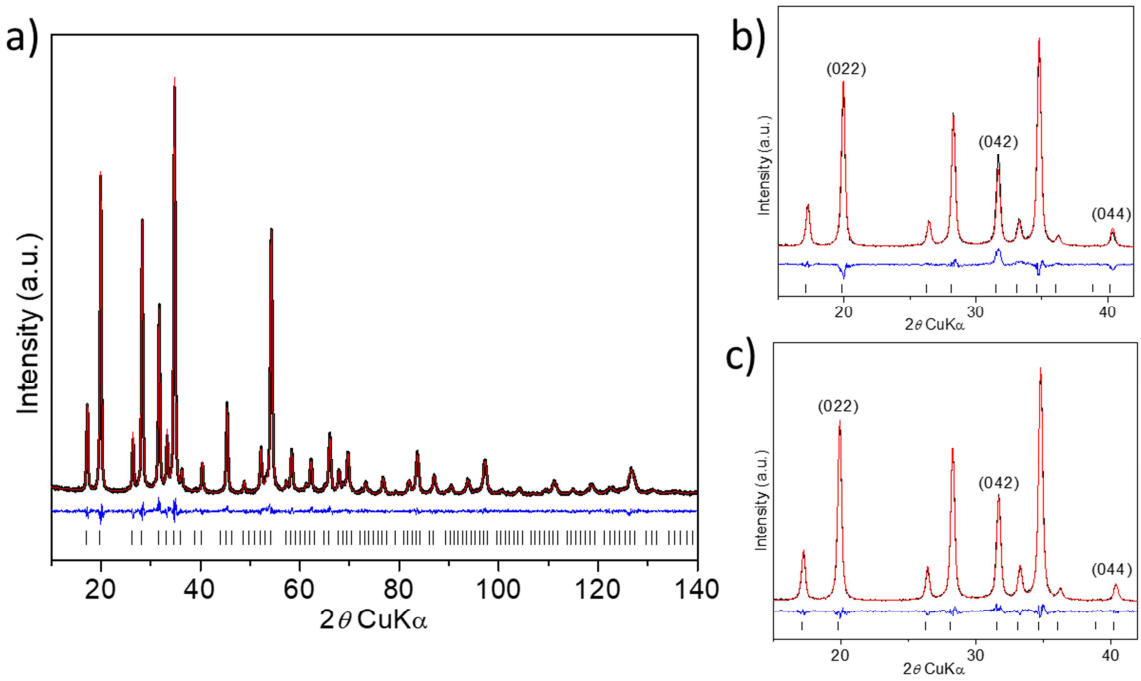

Fig. 1. Rietveld refinement plot of $Na_3Hf_{1.7}Ge_3O_{10}(OH)_{1.8}$ (black curve – experimental; red curve – calculated XRD pattern; blue curve – difference plot; black bars – Bragg peak positions) (a) and details before (b) and after (c) refinement of the occupancy factor of Hf^{4+} cation.

Table 1. Crystal data and structure refinement parameters.

Compound	**$Na_3Hf_{1.7}Ge_3O_{10}(OH)_{1.8}$**
Formula weight (g/mol)	780.84
Crystal system	cubic
Space group	*Ia*-3*d* (no. 230)
Unit cell (Å)	12.6819(2)
Cell volume (Å^3)	2039.65(1)
Z	8
D (g/cm^3)	5.09609
Radiation type	Cu $K\alpha_{1,2}$
2θ range (^{o})	10 – 140
2θ theta step (^{o})	0.04
No. of indep reflns	166
Background	Chebychev polynomial, 15 coefficient
Reliability factors	R_p = 5.39, R_{wp} = 7.26, R_{exp} = 6.10, GOF = 1.19
Structure factor	R_B = 1.50

3. Results and discussion

Fig. 2 shows the refined structure of $Na_3Hf_{1.7}Ge_3O_{10}(OH)_{1.8}$. The framework is composed of alternating, corner-sharing, regular HfO_6 octahedra and GeO_4 tetrahedra. The cavities formed among polyhedra are occupied by Na^+ cations with dodecahedral surrounding. This structural arrangement is typical for the majority of the garnets. Fig.s 1b, c show details of the Rietveld plot before and after refinement of the site occupancy factor of Hf^{4+}. The intensity discrepancy

between the calculated and experimental (042), (022) and (044) reflections before refinement of the site occupancy factor of Hf^{4+} suggested a difference of the electronic density along the atomic planes where reside Hf^{4+} cations (Fig. 2). The better fitting (Fig. 1c) suggested a decreased site occupancy factor of Hf^{4+}, namely existing Hf^{4+} vacancy.

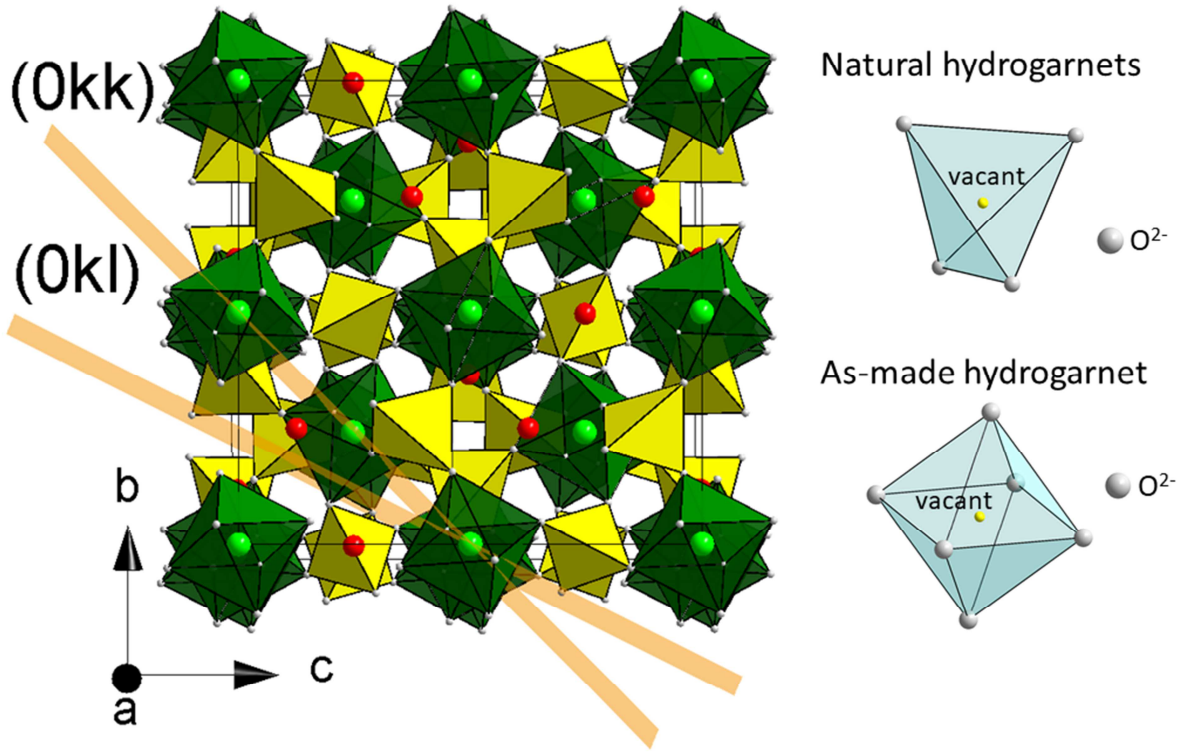

Fig. 2. Crystal structure of $Na_3Hf_{1.7}Ge_3O_{10}(OH)_{1.8}$ (Na cations – red spheres; HfO_6 octahedra – green; GeO_4 tetrahedra – yellow) showing the atomic planes related with the localized structural disorder over the Hf^{4+} cation, and the main difference between the local polyhedral disorder in classical hydrogarnets and as-made phase.

This observation was accompanied by higher isotropic displacement of Hf^{4+} when compared with lighter Na^+ and O^{2-} ions. The attempts to refine the site occupancy of Ge^{4+} and Na^+ showed

no evidence of deviation from the full site occupancy. Increased thermal factor of Ge^{4+} suggested that partly missing hafnium atoms induces isotropic instability in the adjacent tetrahedral site.

Currently, the local structural disorder of hydrogarnets (hydrogrossular, hibschite and katoite) is associated with partial occupancy of the tetrahedral Si^{4+} site [1]. As a result, the missing positive charge is compensated by partial protonation of the oxygen anion that is in the tetrahedral surrounding of the absent cation [18, 19]. Unlike this mechanism, in $Na_3Hf_{1.7}Ge_3O_{10}(OH)_{1.8}$ the tetrahedral Ge^{4+} site is fully occupied and the disorder takes place over the octahedral Hf^{4+} site (Fig. 2). Similar to the natural hydrogarnets, the reduced positive charge is compensated by formation of a hydroxyl group. In the as-synthesized sample, additional contribution to the oxygen protonation is made by the combination of monovalent (A) and tetravalent (B and C) cations residing in dodecahedral, octahedral and tetrahedral sites, respectively. The crystal structure and element combination in this system make mandatory the incorporation of one hydrogen atom in order to compensate the positive charge: $A_3^{+}B_2^{4+}C_3^{4+}O_{12}^{2-}(H^{+})$ (23 positive and 23 negative charges). This scenario is valid for fully occupied dodecahedral, octahedral and tetrahedral sites. In reality, the hydrogen inclusion in $Na_3Hf_{1.7}Ge_3O_{10}(OH)_{1.8}$ is due to the combination of local disorder of the octahedral site and specific chemical composition. Our previous report on the synthesis, crystal structure and optical properties of $Na_3Zr_{1.8}Ge_3O_{10}(OH)_{2.2}$ [8] showed that this suggested mechanism for the inclusion of hydroxyl groups in garnets may not be an isolated case. The obtained bond distances for Hf-O (6 x 2.111 Å), Ge-O (4 x 1.752 Å) and Na-O (4 x 2.498 and 4 x 2.609 Å) (Table S2) are in a fair agreement with the expected values for similar materials [8, 20].

Bond-valence sums (BVSs) [21] calculations for Hf-O gave 3.61 v.u. which is lower than the expected 4.00 v.u. (Table S2). The same calculations made for Na-O and Ge-O bonds resulted in

values of 1.06 and 3.95 v.u. which are not far from the expected 1.00 and 4.00 v.u., respectively (Table S2). These facts strongly support the local structural disorder over the Hf position. BVSs calculations for the oxygen atom gave 1.72 v.u. which is lower than the expected value of 2.00 v.u. and it can be considered as indirect evidence for the presence of hydroxyl group.

Chemical (EDS) analysis resulted in Na : Hf : Ge ratio of 0.6 : 0.6 : 1.0 which is in a good agreement with the Ge/Hf of 1.8 derived from the structural analysis. The lower amount of sodium can be due to its volatile nature which results in losses during the analysis or due to water substituted Na atoms.

In order to examine the hydroxyl species in $Na_3Hf_{1.7}Ge_3O_{10}(OH)_{1.8}$, we compared the FTIR spectra of the as-synthesized and the same sample treated with D_2O (Fig. 3). The crystalline phase remains after D_2O treatment, as confirmed by PXRD. Both spectra show adsorption doublet band of CO_2 at 2360 cm^{-1} [22]. Thus, the absence of typical O-D stretching bands (2150 - 2750 cm^{-1}) is attributed to low concentration of H-O-D molecules [23]. However, the proton exchange reaction could result in clear difference between the relative signal intensities and band positions mainly at the range corresponding to the O-H and H-O-H vibration modes of the two samples [24, 25]. Similar alteration of the band intensity due to protons exchange has been reported for variety of inorganic [23] and organic [26] compounds. In our particular case, the effect of deuteration helps to confirm the presence of strongly connected OH groups whose band intensity has been poorly resolved within the broad band (3470 cm^{-1}) of the as-synthesized sample. Thus, O-H stretching bands at around 3414 and 3471 cm^{-1} are assigned to molecules with distorted H-bonds while the band at around 3551 cm^{-1} is attributed to free O-H stretching or weak hydrogen bonding [23]. The H-O-H bending mode typical for the water molecule appears as a split band – the maximum at 1637 cm^{-1} is attributed to surface adsorbed water and the bands

at 1618 and 1620 cm^{-1} correspond to tightly bounded water molecules [25] that may partly occupy the sodium site. It is to notice that after the treatment with D_2O the contribution to the spectrum from firmly connected water molecules increases which is deduced from the relative difference between the intensity of the two H-O-H bending modes.

The weak band at 613 cm^{-1} is assigned to OH libration mode [27] while the intense bands at 768 and 407/403 cm^{-1} are attributed to Ge-O [28] and Hf-O stretching modes [29], respectively. The frequency shift from 407 to 403 cm^{-1} is attributed to increase of Hf-O(H) bond strength after the treatment with D_2O.

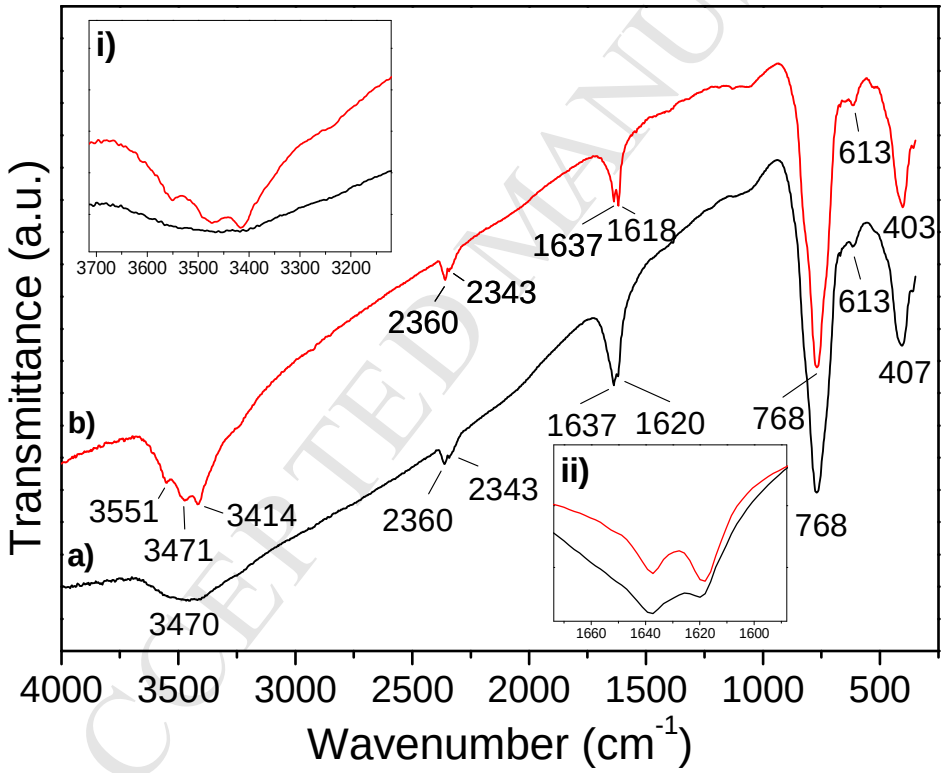

Fig. 3. FTIR spectra of the as-synthesized (a) and D_2O treated (b) $Na_3Hf_{1.7}Ge_3O_{10}(OH)_{1.8}$. The insets show the O-H stretching (i) and H-O-H bending (ii) modes.

TG curve (Fig. 4a) provides additional evidence for the presence of hydroxyl species in the sample. The total mass loss between 25 and 675 ºC (4.4 %) occurs in two steps: (1) between 25 and 125 ^{o}C where the sample losses 1.2 % of its mass, and (2) between 125 and 675 ºC where occurs 3.2 % of the mass loss. The mass loss of step 1 could be due to the surface adsorbed water since the submicron balls are well packed (Fig. 5). Considering that the structurally estimated 1.8 OH groups lose mass in a way: 1.8 OH^{-} → 0.9 H_2O + 0.9 O^{2-} which corresponds to 2.1 % of total mass of the sample, the remaining 1.1 % (around 0.5 H_2O) could be due to the water which partly occupies the dodecahedral site. This is in accordance with EDS results. In fact, the calcination at 680 ºC for 2 hours results in the unit cell shrinkage ($a \approx 12.52$ Å) (Fig. S1).

DSC curve (Fig. 4b) shows three events with different intensity. The first endothermal peak at around 60 ^{o}C is attributed to dehydration due to the removal of weakly bonded surface water. The second peak is exothermic and appears at around 300 ^{o}C. It is assigned to lattice relaxation due to rearrangement of structural defects. The third peak at around 400 ^{o}C is endothermic and it is attributed to release of strongly bonded water and hydroxyl groups.

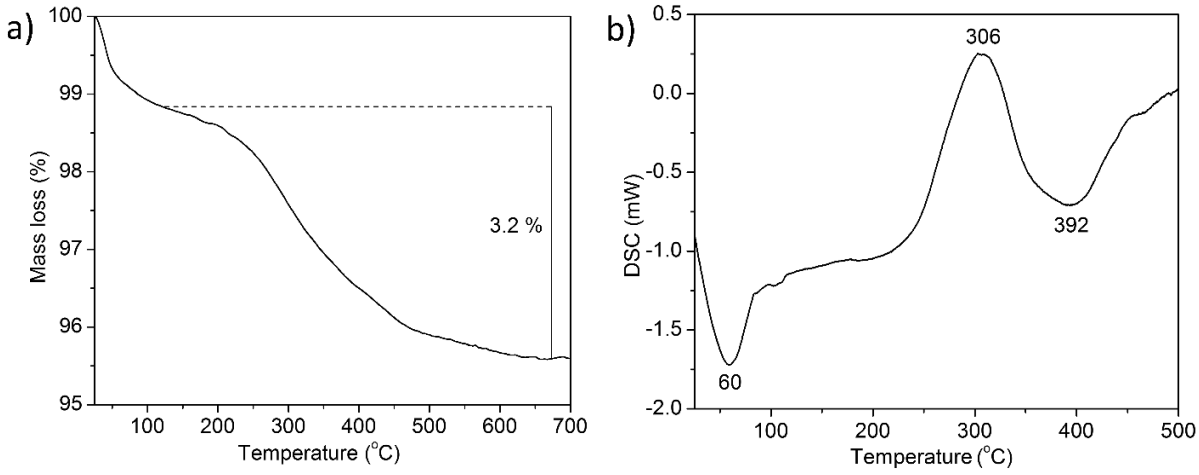

Fig. 4. TG (a) and DSC (b) curves of the as-synthesized $Na_3Hf_{1.7}Ge_3O_{10}(OH)_{1.8}$.

Fig. 5 shows SEM image of the as-synthesized $Na_3Hf_{1.7}Ge_3O_{10}(OH)_{1.8}$. The crystallites appear as separated ball-like particles (100-600 nm). This is slightly different to the one of $Na_3Zr_{1.8}Ge_3O_{10}(OH)_{2.2}$ where similar size ball-like particles form densely packed aggregates.

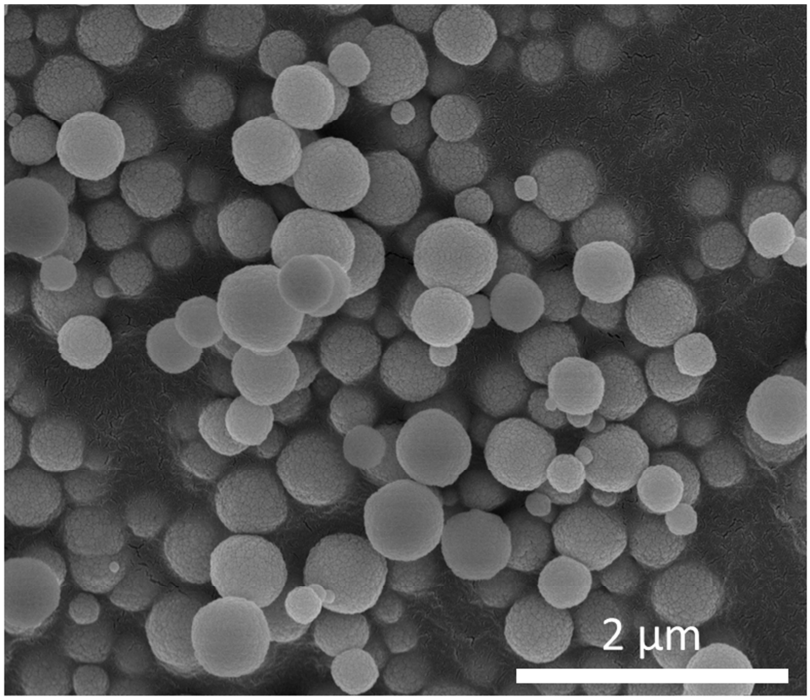

Fig. 5. SEM image of the as-synthesized $Na_3Hf_{1.7}Ge_3O_{10}(OH)_{1.8}$.

4. Conclusions

This work reveals the first hafnium germanate with garnet-type of structure. The synthesis and structure analysis of $Na_3Hf_{1.7}Ge_3O_{10}(OH)_{1.8}$ show potentially large group of hydrogarnets where the inclusion of hydroxyl groups is based on novel mechanism when compared to any of known hydrated garnets. Namely, local disorder over the octahedral cation position in combination with specific chemical composition ($A_3^{+}B_2^{4+}C_{3-x}^{4+}O_{12-x}^{2-}H_{1+2x}^{+}$, where the dodecahedral A site is occupied only by monovalent while the octahedral B and tetrahedral C sites are tetravalent cations) triggers charge disbalance compensated by partial protonation of the oxygen anion.

Acknowledgements

This work was supported by the Portuguese Foundation for Science and Technology (IF/01516/2013 and UID/CTM/50011/2013).

Appendix A. Supplementary data

References

[1] E.S. Grew, A.J. Locock, S.J. Mills, I.O. Galuskina, E.V. Galuskin, U. Halenius, Nomenclature of the garnet supergroup, Am Mineral 98(4) (2013) 785-810.

[2] E.F. Baxter, M.J. Caddick, B. Dragovic, Garnet: A Rock-forming mineral petrochronometer, petrochronology: methods and applications Reviews in Mineralogy and Geochemistry 83(1) (2017) 469-533.

[3] A. Tauber, C.G. Whinfrey, E. Banks, The crystal chemistry of some germanium garnets, Journal of Physics and Chemistry of Solids 21(1-2) (1961) 25-32.

[4] S. Geller, Crystal chemistry of garnets, Zeitschrift Fur Kristallographie, Bd. 125 (1967) S. 1-47.

[5] J.P.M. Damen, J.A. Pistorius, J.M. Robertson, Calcium gallium germanium garnet as a substrate for magnetic-bubble application, Materials Research Bulletin 12(1) (1977) 73-77.

[6] G. Blasse, J. Deblank, D.J.W. Ijdo, The luminescence of the garnet $Ca_4ZrGe_3O_{12}$, Materials Research Bulletin 30(7) (1995) 845-850.

[7] S. Nagat, M. Uemura, T. Orluchl, M. Sakuraoka, J. Awaka, S. Ebisu, Magnetic susceptibility of several germanium garnets, Physica B-Condensed Matter 398(1) (2007) 85-88.

[8] S. Ferdov, R.A.S. Ferreira, Z. Lin, Z.Y. Wu, Mild hydrothermal synthesis, crystal structure, photoluminescence properties and emission quantum yield of a new zirconium germanate with garnet-type structure, Journal of Solid State Chemistry 190 (2012) 18-23.

[9] C.Y. Liu, Z.G. Xia, M.S. Molokeev, Q.L. Liu, Synthesis, crystal structure, and enhanced luminescence of garnet-type $Ca_3Ga_2Ge_3O_{12}:Cr^{3+}$ by codoping Bi^{3+}, Journal of the American Ceramic Society 98(6) (2015) 1870-1876.

[10] V.D. Zhuravlev, A.P. Tyutyunnik, N.I. Lobachevskaya, Preparation and crystal structure of garnet-type calcium zirconium germanate $Ca_4ZrGe_3O_{12}$, Powder Diffraction 31(4) (2016) 292-294.

[11] V.D. Zhuravlev, N.I. Lobachevskaya, Y.A. Velikodnyi, L.V. Ermakova, V.G. Bamburov, New vanadium germanium garnets, Doklady Chemistry 479 (2018) 45-48.

[12] Y. Tokudome, K. Fujita, K. Nakanishi, K. Kanamori, K. Miura, K. Hirao, T. Hanada, Sol-gel synthesis of macroporous YAG from ionic precursors via phase separation route, Journal of the Ceramic Society of Japan 115(1348) (2007) 925-928.

[13] M. Mookherjee, High-pressure elasticity of sodium majorite garnet, $Na_2MgSi_5O_{12}$, Am Mineral 99(11-12) (2014) 2416-2423.

[14] B. Wedel, K. Sugiyama, Crystal structure of sodium iron aluminium tellurate, a new tellurium compound with garnet structure, $Na_3(Fe,Al)_3Te_2O_{12}$, Zeitschrift fur Kristallographie - New Crystal Structures 214(2) (1999) 151-152.

[15] A. Altomare, C. Giacovazzo, A. Guagliardi, A.G.G. Moliterni, R. Rizzi, P.E. Werner, New techniques for indexing: N-TREOR in EXPO, Journal of Applied Crystallography 33(4) (2000) 1180-1186.

[16] A. Altomare, M.C. Burla, M. Camalli, B. Carrozzini, G.L. Cascarano, C. Giacovazzo, A. Guagliardi, A.G.G. Moliterni, G. Polidori, R. Rizzi, EXPO: a program for full powder pattern decomposition and crystal structure solution, Journal of Applied Crystallography 32 (1999) 339-340.

[17] A. Le Bail, Whole powder pattern decomposition methods and applications: A retrospection, Powder Diffraction 20(4) (2005) 316-326.

[18] O. Ferro, E. Galli, G. Papp, S. Quartieri, S. Szakáll, G. Vezzalini, A new occurrence of katoite and re-examination of the hydrogrossular group, European Journal of Mineralogy 15(2) (2003) 419-426.

[19] G.A. Lager, T. Armbruster, F.J. Rotella, G.R. Rossman, OH substitution in garnets: X-ray and neutron diffraction, infrared, and geometric-modeling studies, Am Mineral 74(7-8) (1989) 840-851.

[20] G.D. Ilyushin, Hydrothermal crystallization and crystal-structure of ionic conductor $Na_4Hf_2Ge_3O_{12}$ (Nasicon), Kristallografiya 34(4) (1989) 839-845.

[21] M.W. Lufaso, P.M. Woodward, Prediction of the crystal structures of perovskites using the software program SPuDS, Acta Crystallographica Section B: Structural Science 57(6) (2001) 725-738.

[22] R.W. Stevens, R.V. Siriwardane, J. Logan, In situ Fourier transform infrared (FTIR) investigation of CO_2 adsorption onto zeolite materials, Energ Fuel 22(5) (2008) 3070-3079.

[23] Z.S. Nickolov, J.D. Miller, Water structure in aqueous solutions of alkali halide salts: FTIR spectroscopy of the OD stretching band, J Colloid Interf Sci 287(2) (2005) 572-580.

[24] A. Beran, OH groups in nominally anhydrous framework structures - an infrared spectroscopic investigation of danburite and labradorite, Physics and Chemistry of Minerals 14(5) (1987) 441-445.

[25] J.L. Bishop, C.M. Pieters, J.O. Edwards, Infrared spectroscopic analyses on the nature of water in montmorillonite, Clay Clay Miner 42(6) (1994) 702-716.

[26] C.M. Phillippi, K.S. Mazdiyasni, Infrared and Raman spectra of zirconia polymorphs, Journal of the American Ceramic Society 54(5) (1971) 254-258.

[27] S. Yariv, Hellerka.L, I.R. evidence for migration of protons in H-montmorillonites and organo-montmorillonites, Clay Clay Miner 21(3) (1973) 199-200.

[28] K. Senda, K. Ishida, D.M. Jenkins, X-ray Rietveld refinement and FTIR spectra of synthetic (Si,Ge)-richterites, Am Mineral 90(7) (2005) 1062-1071.

[29] X. F. Wang, L. Andrews, Infrared spectrum and structure of the $Hf(OH)_4$ molecule. Inorganic Chemistry 44(20) (2005) 7189-7193.

The first hafnium germanate with garnet-type of structure reveals a novel mechanism for hydroxyl inclusion.